where N is the demagnetization factor, γ is 2.8 Mc/oersted, M is the magnetization, and H_A is the applied field. The demagnetization factor is negligible in the direction that the ferrite is relatively thick and the surface is small. Therefore, for a thin ferrite disc, N_X and N_Y are zero then

$$H_A = \frac{f}{\gamma} + 4\pi M. \quad (3)$$

Below-resonance circulators with low insertion loss can be built for frequencies as low as about 750 Mc/s using available materials with a saturation magnetization of approximately 300 gauss.

For frequencies below 750 Mc/s, the above resonance operation is utilized for low insertion loss circulators.

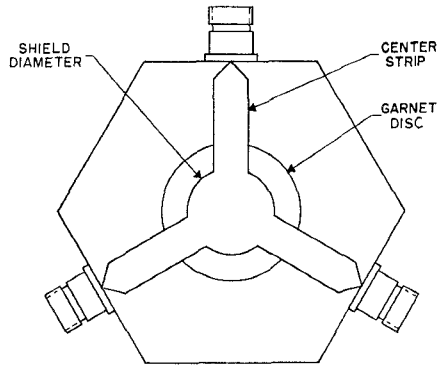

Fig. 1. Strip-line circulator at 150 Mc/s.

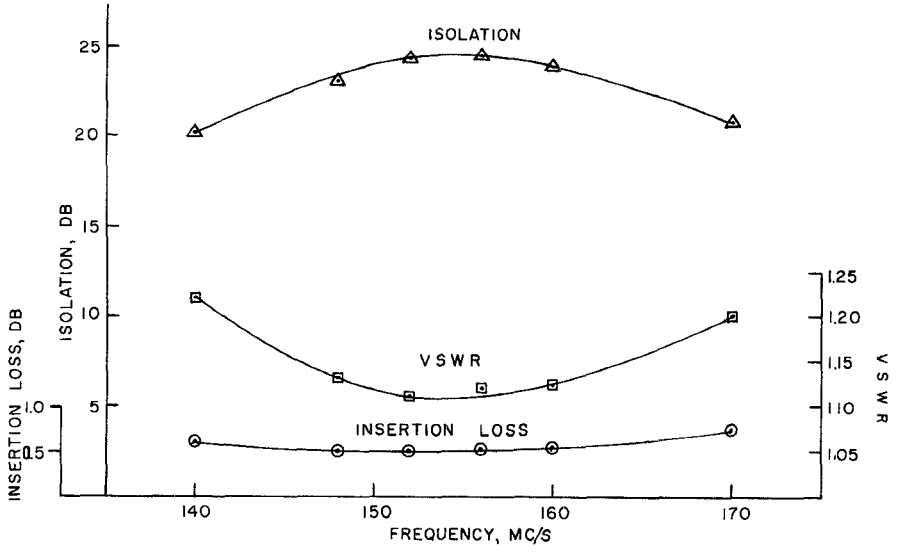

Fig. 2. Characteristics of 150 Mc/s circulator.

Buehler and Eikenberg[1] reported strip-line circulators for the 100 to 400 Mc/s region utilizing a magnesium ferrite with a Curie temperature of 100°C. For high-temperature performance, garnet materials have demonstrated a more satisfactory performance.

For above-resonance low insertion loss circulators, the required applied field is

$$H_A = \frac{f}{\gamma} + 4\pi M + n\Delta H \quad (4)$$

for $n=2$ which is the biasing point at two line widths above resonance; losses are sufficiently low.

Figure 1 shows the structure of a 150 Mc/s strip-line circulator using an Airtron garnet material. It was found empirically that the characteristics of the circulator can be optimized for $D_f/D_s=1.8$ where D_f is the ferrite diameter and D_s is the shield diameter.

Figure 2 shows the characteristics of this circulator. An isolation greater than 20 dB and an insertion loss of less than 0.75 dB was achieved over a 20 percent band without use of a direct matching element.

The input impedance of the circulator plotted on a Smith chart indicated that a better match can be obtained by adding an inductive reactance before the ferrite disks. This inductive structure was introduced by reducing the width of the center conductor.

The characteristics of the circulator were improved and a return loss greater than 30 dB was measured, however; a reduction in bandwidth was observed. The high power requirement of the unit limited the type of matching structure which could be utilized.

Temperature Consideration: When the circulator is subjected to a high temperature environment, the saturation magnetization of the garnet will decrease. The change in saturation magnetization is much greater for the substituted magnesium manganese ferrites; nevertheless, to compensate for this reduction in saturation magnetization, (3) shows that the applied magnetic field should be reduced. In practice, this is achieved by using a compensating steel in series with the magnetic circuit. The permeability of the compensator reduces with an increase of temperature. This scheme is effective for low temperature as well.

For above-resonance circulators, the insertion loss increases rapidly with a reduction in temperature. Equation (3) shows that when $4\pi M$ is increased, the resonance frequency is shifted down, which would lower the insertion loss. However, the increase in insertion loss is due to broader line width.

The authors would like to acknowledge many helpful discussions with Dr. E. Wantuch.

B. Maher
D. Mitchell
A. Reeves
Airtron
Division of Litton
Precision Products, Inc.
Morris Plains, N. J.

Frequency Doublers Using Varactors Exhibiting "Punch-Through" Capacitance-Voltage Behavior

Recently, a number of authors[1-5] have given the analysis of the overdriven doubler for abrupt-junction, graded-junction, and stepwise-junction varactor doublers. All previous work has stimulated considerable interest in the prediction of power and efficiency of frequency doublers using varactors exhibiting a general nonlinearity. This discussion is concerned with the detailed analysis of the "punch-through" behavior varactor doubler to determine the conditions of optimum input and output resistances, maximum conversion efficiency, and power. The results will generally be determined by numerical techniques because of the algebraic complexity of the solutions. The analysis in this discussion asumes the varactor to be imbedded in a lossless tuned circuit.

Scarlett[1] and Rafuse[2] have made detailed analyses of the overdriven stepwise-junction varactor doubler and also point out that such an "ideal" diode will not multiply unless it is overdriven. In no case was a diode actually found to have such a stepwise-junction. However, varactors exhibiting "punch-through" capacitance-voltage behavior can usually be obtained. The broken line in Fig. 1 represents a stepwise-junction which has a constant elastance in the range of $0<q+q_\phi\leq Q_B+q_\phi$ and the solid curve

Manuscript received June 17, 1965, revised August 26, 1965.

[1] G. V. Buehler and A. F. Eikenberg, "Stripline Y-circulators for the 100 to 400 Mc region," *Proc. IRE*, vol. 49, pp. 518–519, February 1961.

[1] R. M. Scarlett, "Harmonic generation with a capacitor exhibiting an abrupt capacitance change," *Proc. IEEE (Correspondence)*, vol. 52, pp. 612–613, May 1964.

[2] R. Rafuse, "Recent development in parametric multipliers," Research Lab. of Electronics, M.I.T., Cambridge, Mass., Quarterly Progress Rept. 72, pp. 281–293, January 15, 1964.

[3] C. B. Burckhardt, "Analysis of varactor frequency multipliers for arbitrary capacitance variation and drive level," *Bell Sys. Tech. J.*, vol. 44, pp. 675–692, April 1965.

[4] J. A. Davis, "The forward-driven varactor frequency doubler," S.M. Thesis, Dept. of Elec. Engrg., M.I.T., Cambridge, Mass., May 1963.

[5] A. I. Grayzel, "Greater doubler efficiency using varactor diodes with small values of gamma," *Proc. IEEE (Correspondence)*, vol. 53, pp. 505–506, May 1965.

represents "punch-through" behavior. The characteristic of "punch-through" behavior is observed in junctions formed with epitaxial material. It is actually caused by some of the depletion layer encountering the highly doped substrate layer at some voltage less than breakdown. Therefore, the majority of the elastance change takes place in the lower reverse voltage region. Practically no change in elastance occurs in the higher reverse voltage region. This discussion will point out that the efficiency of a frequency doubler using a "punch-through" behavior varactor appears to be superior in some respects to that of an abrupt-junction varactor.

This analysis is based on a simplified varactor model which has a voltage-independent series resistance R_s and no bulk and contact resistance associated with its active region. Figure 2 shows that the logarithm of the capacitance-voltage relationship of a "punch-through" varactor is dependent on the slope γ_1 in region 1 and γ_2 in region 3. The slope of the C-V curve in region 2 varies continuously from γ_1 to γ_2. For mathematical convenience, the C-V curve in region 2 has broken line approximation. Hence, the charge in the varactor can be written approximately:

$$q(\nu) + q_\phi = \frac{(V_{bp} + \phi)^{\gamma_1} C_{bp}}{(1 - \gamma_1)} (V + \phi)^{1-\gamma_1}$$

$$\text{for } 0 < V \leq V_{bp} \quad \text{(1a)}$$

$$q(\nu) + q_\phi = \frac{(V_B + \phi)^{\gamma_2} C_{\min}}{(1 - \gamma_2)} ((V + \phi^{1-\gamma_2}) - (V_{bp} + \phi)^{1-\gamma_2}) + \frac{(V_{bp} + \phi) C_{bp}}{1 - \gamma_1}$$

$$\text{for } V_{bp} < V < V_B \quad \text{(1b)}$$

where

C_{bp} = the capacitance at the break point
V_{bp} = the voltage at the break point
$C_{\min} = S_{\max}^{-1}$ = minimum capacitance at the varactor breakdown voltage
V_B = the varactor breakdown voltage
ϕ = the varactor electrostatic potential
q_ϕ = the charge at the varactor electrostatic potential.

The relationship between the normalized charge $\hat{q}_{bp}$ and voltage $\hat{V}_{bp}$ at the break point with respect to the different slopes of γ_1 and γ_2 can be derived from (1a) and (1b) and is plotted in Fig. 3.

$$\hat{V}_{bp} = \frac{V_{bp} + \phi}{V_B + \phi} = \left[\frac{1 - \gamma_2}{1 - \gamma_1}\left(\frac{1}{\hat{q}_{bp}} - 1\right) + 1\right]^{-1/1-\gamma_2} \quad (2)$$

where

$$\hat{q}_{bp} = \frac{q_{bp} + q_\phi}{Q_B + q_\phi}.$$

Now it is a straightforward matter to compute numerically the input power of the fundamental frequency ω_0 for the varactor, assuming that the normalized charge $\hat{q}$ operates in the region between breakdown voltage to forward-biased conduction containing no harmonics higher than second harmonic and that $\hat{q}_1 = 2\hat{q}_2$.[6,7] The maximum input converted power is then given by:

$$P_{\text{in}} = A\omega_0 C_{\min}(V_B + \phi)^2 \quad (3)$$

The conversion efficiency can be written as:

$$\eta = 1 - h\frac{\omega_0}{\omega_c}. \quad (4)$$

The input and load resistances are given by:

$$R_{\text{in}} = R_{\text{load}} = \frac{2}{h}\frac{1}{\omega_0 C_{\min}}. \quad (5)$$

The coefficients of A and h were solved numerically on an IBM 1620 digital computer in a region from 0.1 to 1 of the normalized charge at the break point. Graphs illustrating some of the results are given in Fig. 4. The coefficients of A with $\hat{q}_1/\hat{q}_2$ equal to 2.25 and 1.88 have also been solved numerically by computer and are less than that of $\hat{q}_1/\hat{q}_2$ equal to 2. It is evident that the coefficients of A with $\hat{q}_1/\hat{q}_2$ equal to 2 give a good approximation.

In Fig. 4, values of A and h are plotted against the normalized charge at the break point with γ_1 equal to $\frac{1}{2}$ and various values of γ_2. The points at $\hat{q}_{bp} = 1$ are abrupt-junction-varactor doubler results which have been given by Penfield and Rafuse.[7] It is clear from Fig. 4 that the conversion efficiency represents an improvement when $\hat{q}_{bp}$ lies in the range 0.55 to 0.9 and will reduce rapidly when $\hat{q}_{bp}$ is less than 0.4 and beyond 0.95. The change of $h - \hat{q}_{bp}$ plots appears more reasonable physically in the region $\hat{q}_{bp} < 0.3$ because the γ_2 region now dominates. A further conclusion is evident from the $A - \hat{q}_{bp}$ plots in Fig. 4. The power handling capability when $\hat{q}_{bp}$ equals 0.6 and γ_2 equals 0 differs only slightly from that of the abrupt-junction-varactor doubler.

The results given in this analysis indicate that the highest efficiency occurs when the "punch-through" varactor $\hat{q}_{bp}$ is in the range 0.55 to 0.8, and that the power handling capability is highest when $\hat{q}_{bp}$ is between 0.8 to 1 but decreases as $\hat{q}_{bp}$ decreases. Figure 4 shows that a break-point charge of 0.7 to 0.95 improves both the efficiency and power handling capability of a doubler using a varactor with $\gamma_1 = \frac{1}{2}$ and $\gamma_2 = 0$. Table I compares the coefficients of h and A for $\frac{1}{2}$-power and $\frac{1}{3}$-power "punch-through" be-

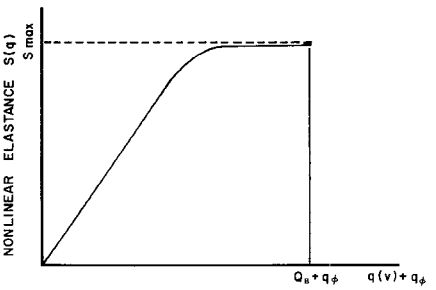

Fig. 1. Stepwise and "punch-through" nonlinear elastance characteristics.

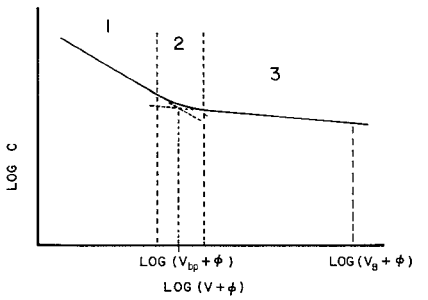

Fig. 2. "Punch-through" behavior varactor C-V characteristic.

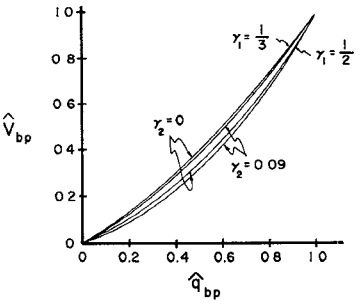

Fig. 3. Normalized charge vs. normalized voltage at the break point for various values of γ_1 and γ_2.

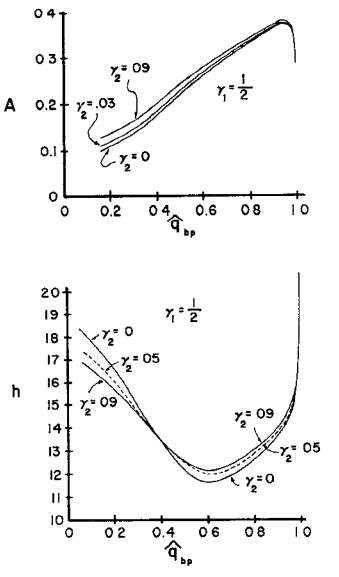

Fig. 4. Plot of A and h as a function of $\hat{q}_{bp}$ for $\gamma_1 = 1/2$ and various values of γ_2.

TABLE I

COMPARISON OF THE COEFFICIENTS OF h AND A FOR "PUNCH-THROUGH" BEHAVIOR VARACTOR, ABRUPT-JUNCTION, AND OVERDRIVEN STEPWISE-JUNCTION DOUBLERS

Parameter	"Punch-through" behavior varactor with $\lambda_2 = 0$, $\hat{q}_{bp} = 0.6$		Abrupt-junction [7]	Overdriven stepwise-junction [1]
	$\gamma_1 = 1.2$ nominal drive	$\gamma_1 = 1.3$ nominal drive	nominal drive	drive = 2
h	11.6301	13.4545	20.8000	9.4247
A	0.0260	0.0173	0.0285	0.0629

[6] T. C. Leonard, "Prediction of power and efficiency of frequency doublers using varactors exhibiting a general nonlinearity," *Proc. IEEE*, vol. 51, pp. 1135–1139, August 1963.

[7] P. Penfield, Jr., and R. Rafuse, *Varactor Applications*. Cambridge, Mass.: M.I.T. Tech. Press, 1962, pp. 316–345 and 603–614.

havior varactor, abrupt-junction, and overdriven stepwise-junction doublers. It is known that the $\frac{1}{2}$-power "punch-through" varactor exhibits a higher conversion efficiency in doublers than does the $\frac{1}{3}$-power "punch-through" varactor. In general, this increase in efficiency for nominal drive is pronounced for a varactor having "punch-through" behavior. Note that the analysis described here is based on a normally driven condition. Furthermore, the efficiency of an overdriven varactor doubler or a higher-order harmonic generator can also be enhanced by using the "punch-through" behavior varactor. Logical future work would be the analysis of higher-order multipliers using "punch-through" varactors.

CHENG LEE CHAO[8]
Applied Research Lab.
Sylvania Electronics Systems
Div. of Sylvania Elec. Prods., Inc.
Waltham, Mass.

[8] Formerly with Varian Associates, Beverly, Mass.

A Digital Current Controlled Latching Ferrite Phase Shifter

INTRODUCTION

With increased interest being placed on phased array antenna systems, much effort is being extended to improve the component phase shifters. The recent development of digital "latching ferrite" devices has been of considerable significance.[1-4] Such phase shifters, for example, have reduced switching speeds to microsecond or submicrosecond intervals and have no need for bulky switching coils. This correspondence is concerned with the design of a new latching device which obtains digital increments of phase shift by using material properties exhibited in a single element geometry.

In present designs, four, five, or six ferrimagnetic toroids of various lengths are placed in a waveguide configuration as shown in Fig. 1(a). Quarter-wave matching transformers are included at either end of the series while dielectric separators are placed between adjacent elements. As indicated, a separate dc current path is provided through each toroid. When rather narrow, full waveguide height toroids are used, it is found that this configuration simulates the widely used twin slab, nonreciprocal phase shifter design.[2]

Digital increments of phase shifts are obtained in these designs by switching the magnetization of the component toroids between remanent states. Typical operating characteristics for a present C-band latching phase shifter are listed in Table I.[2] As indicated, such phase shifters offer many desirable characteristics; however, the necessity of having a separate driver for each element and the necessity of including somewhat lossy dielectric separators are undesirable features.

DESIGN OF NEW PHASE SHIFTER

The new design consists basically of a single toroid placed in a waveguide as shown in Fig. 1(b). In this configuration the toroid's length is chosen to give a nominal 360° differential phase shift when switched between remanent states. Intermediate steps of differential phase shift are obtained by using partial demagnetization of the toroid core.

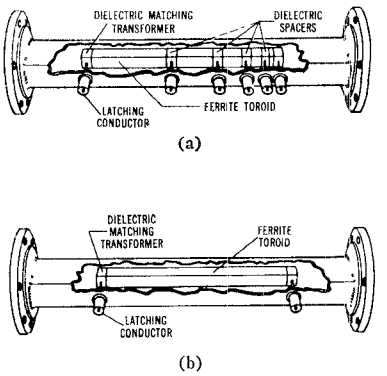

Fig. 1. Assembled view of (a) present five-bit latching ferrite phase shifter and (b) new single-toroid design.

TABLE I
CHARACTERISTICS OF TYPICAL FIVE-BIT PHASE SHIFTER

Frequency	5.4–5.9 Gc/s	Switching Speed	≤ 0.2 μs
Phase Deviation	3 percent deviation over band	Insertion Loss	<0.80 dB
Size	$1\frac{1}{2}'' \times \frac{3}{4}'' \times 8''$	VSWR	<1.5
Switching Energy	<300 μ joules per pulse /180° bit <0.120 watts at 400 pps	RF Power Capacity	>10 kw

If it is assumed that the toroidal material has the major hysteresis loop depicted in Fig. 2, the operation of both the present multi-element and the new design may be examined by considering this loop. For a present design, suppose the toroid is initially in a reference state A'. Then, if a large positive current pulse is passed through the toroid, the material will saturate and retain a positive residual induction, point A. A corresponding differential phase shift is obtained.

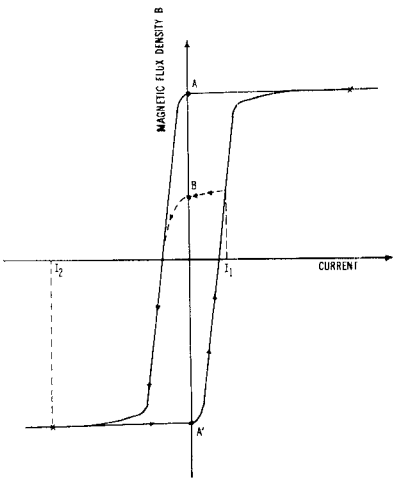

Fig. 2. Hysteresis loop for material used.

In the new design, this process is altered somewhat. As before, the toroid is assumed to be initially in a state corresponding to point A'. However, this time a controlled pulse of amplitude I_1 is applied. An intermediate amount of differential phase shift will result (point B). If it is desired to obtain a different value of differential phase shift, a large negative reset pulse of sufficient amplitude (I_2) to assure saturation in the opposite direction needs to be applied. This assures repeatability and eliminates accumulative errors after several switching operations. After this reset current pulse has been applied, a positive pulse of suitable amplitude follows. This process can then be repeated. A curve relating pulse amplitude to degrees of phase shift for a garnet configuration is shown in Fig. 3. A variation of differential phase shift of less than one percent has been obtained experimentally after cycling the toroid several hundred times.

It has been pointed out in the literature that when ferrite toroids are switched between remanence and a largely demagnetized state the switching time will be somewhat longer than when switched between

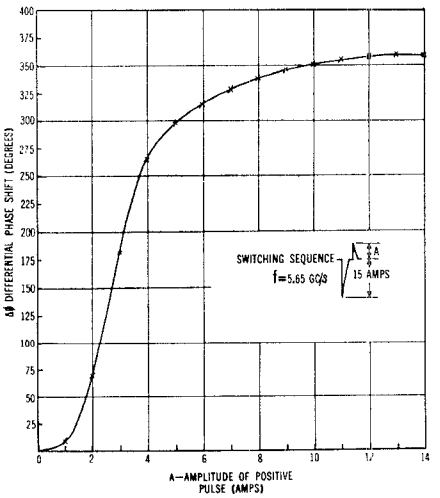

Fig. 3. Amount of the differential phase shift obtained for various amplitudes of positive pulses.

Manuscript received April 15, 1965, revised August 27, 1965.

[1] G. S. Blevins, J. A. Kempic, and R. R. Jones, "C-band digital ferrite phase shifter" (Classified Paper), presented at 1964 Symp. on Electronically scanned Array Techniques and Applications, Rome Air Development Center.

[2] J. A. Kempic and R. R. Jones, "High power C-band phase shifter," Westinghouse Electric Corp., Baltimore, Md., First Quarterly Rept., Contract DA-28-043-AMC-00228; January 1965.

[3] D. R. Taft, "Development of a digital phase shifter using square loop garnet materials," presented at the 1964 Magnetism and Magnetic Materials Conf.

[4] L. R. Whicker and R. R. Jones, "A digital latching ferrite strip transmission line phase shifter," *IEEE Trans. on Microwave Theory and Techniques*, vol. MTT-13, pp. 781–784, November 1965.